Journal of the European Ceramic Society **15** (1995) 201–207
Elsevier Science Limited
Printed in Great Britain
0955-2219/95/$9.50

Determining the Fracture Toughness of Brittle Materials by Hertzian Indentation

P. D. Warren

Department of Materials, Oxford University, Parks Road, Oxford OX1 3PH, UK

(Received 21 December 1993; revised version received 14 July 1994; accepted 1 August 1994)

Abstract

The use of Hertzian indentation as a method for determining the fracture toughness of any brittle material is described. The advantage of the method described here is that the only quantity to be measured is a fracture load. Experimental determinations of K_{IC} *for soda-lime glass and high-purity alumina give results 0·71 and 3·72 MPa* $m^{1/2}$*, respectively.*

Introduction

The fracture toughness of a brittle material is one of its most important mechanical properties. Determination of this value is frequently a complicated process involving preparation of specimens with well-defined sharp cracks of known length. A recent review article[1] has presented a summary of available techniques. However, one method was conspicuous by its absence—that of Hertzian indentation. It is the purpose of this paper to suggest that this method should be looked at afresh.

Indentation techniques in general have certain advantages compared with the more conventional methods: the experimental procedure is straightforward, involving minimal specimen preparation, and the amount of material needed is small. The Vickers indentation method[2–4] is well known. However, it is not without drawbacks. There are now a very large number of theoretical models in the literature (19 are reviewed by Ponton and Rawlings[5,6]) relating the surface crack length measured after indentation to the indenter load and material parameters—Young's modulus, hardness and fracture toughness. There is still considerable debate as to the nature of the cracks observed around a Vickers indentation—the idealised 'half-penny' characteristics of the median/radial system, as opposed to Palmqvist cracking. Cook and Pharr[7] have presented a considerable amount of evidence to suggest that *radial* cracks form almost immediately on loading in a wide variety of crystalline solids. There is also debate on how to determine the type of cracking from the surface-crack length vs applied load relation. For a spirited discussion of these matters the articles by Li *et al.*[8,9] and Srinivasan and Scattergood[10] should be consulted. It should be noted, however, that Lawn[11] asserts that Palmqvist cracks '. . . retain the essential half-penny character.'

Many attempts have been made to use Hertzian indentation—where a hard sphere is pressed into the flat surface of a brittle substrate—to determine K_{IC} for brittle materials: work by Frank and Lawn—glass,[12] by Powell and Tabor—TiC,[13] by Wilshaw—glass,[14] by Nadeau—vitreous carbon,[15] by Warren—TiC, ZrC, VC and WC,[16] by Matzke *et al.*—UO_2,[17] by Matzke—ThO_2,[18] by Inoue and Matzke—ThO_2,[19] by Matzke and Warren—ThO_2,[20] by Matzke and Politis—NbC, Nb(C,N) and NbN,[21] by Matzke *et al.*—(U,Pu)C and (U,Pu)(C,N),[22] by Laugier—TiN coatings on WC–Co,[23] Al_2O_3—ZrO_2,[24] various Al_2O_3—ZrO_2 composites and Sialons,[25] various WC–Co composites[26] and finally, by Zeng *et al.*—glass, Al_2O_3 and Al_2O_3–SiC composites.[27,28]

Broadly speaking, the early work, prior to 1978, used the theory of Frank and Lawn,[12] which strictly only applies for ring-cracks initiating exactly at the edge of the contact zone. The papers by Warren and co-workers,[16–19,21,22] (and those of Laugier[23–26]) used Warren's theory,[16] which involves measuring the radius of the ring-crack seen on the surface after fracture: Matzke and Warren[20] and the recent work by Zeng *et al.*[27,28] involved the cross-sectioning of the specimens after fracture to determine the *depth* of the cone crack. The results obtained so far have been variable. Almond *et al.*[29] point out that the values obtained by Warren[16] on various metal carbides are significantly lower than conventional values; Laugier,[26] on the other hand, for various WC—Co composites, found values considerably higher. This poor agreement may be one reason why the test is not more commonly used. This is a pity because the Hertzian indentation test has at least one considerable advantage over Vickers indentation: until fracture occurs around the indenter the deformation of the substrate is entirely elastic (unless spheres of very small radius, <1 mm, are used). This means that the complications associated with the residual stresses in the Vickers indentation technique do not exist. Furthermore, the elastic stress field is well known.[30]

The disadvantages in the method may be due to the following factors: (i) the stress gradients in the Hertzian field are very steep so that it is difficult to obtain accurate estimates for stress-intensity factors for cracks driven by Hertzian loading; (ii) the results of the analysis are extremely sensitive to the value of Poisson's ratio of the substrate, and (iii) a number of previous experimental determinations of fracture toughness have ignored the effects of elastic mismatch (and friction at the indenter–substrate interface) when the sphere and the substrate are made of elastically dissimilar materials. Much work has been done using either steel or tungsten carbide spheres on glass substrates and there is good experimental evidence[31] that the effects of this significant elastic mismatch on the observed fracture loads are *not* negligible.

Below, we summarise the main aspects of the theory of Hertzian fracture and present a method which enables the value of K_{IC} to be found for any brittle material, as long as it is indented by a sphere made of the same material. The method described here is extremely easy to use, does not require measurement of the ring-crack size and gives reliable results.

Theory

Figure 1 shows a sphere (radius R, elastic constants ν_I, E_I) pressed by a load P into a flat substrate (with elastic constants ν, E). The load is supported over a circular area whose radius, a, is given by:[32]

$$a = \left(\frac{3RP}{4E^*}\right)^{1/3} \tag{1}$$

where:

$$\frac{1}{E^*} = \frac{1-\nu^2}{E} + \frac{1-\nu_I^2}{E_I} \tag{2}$$

The peak pressure under the sphere, p_o, is given by:

$$p_o = \frac{3P}{2\pi a^2} \tag{3}$$

The stress field outside the contact zone has a tensile radial stress near to the surface which

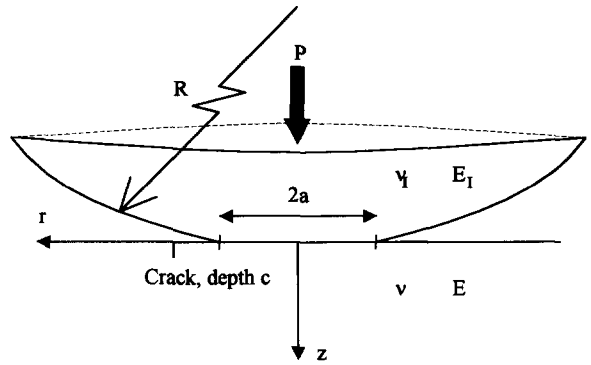

Fig. 1. The geometry of Hertzian contact.

rapidly decreases, and soon becomes compressive, with depth. Thus calculating the stress intensity factors for surface-breaking cracks is not trivial. For short cracks (i.e. those whose depth is less than $a/10$) lying perpendicular to the free surface the method of Nowell and Hills[33] (employing distributed dislocations) can be used to derive expressions for the mode I (and mode II) stress intensity factors. This approach differs from previous work[12,14,16,27,28,34] where it was assumed that the crack path initially lay along the trajectory of the minimum principal stress; here, the pre-cursor flaws are assumed to be perpendicular to the surface; this will tend to *reduce* the K_I values derived here compared to previous results. The use of the method of distributed dislocations enables the effects of the free surface to be accounted for; this will tend to *increase* the K_I values. In this method, a short plane crack of depth c, normal to the free surface, is placed close to the contact zone. The state of stress in the crack's absence is found. When the crack is inserted, unsatisfied tractions appear along the line of the crack. These may be cancelled by the application of equal and opposite tractions along the crack faces, which may be generated by installing a distribution of dislocations. (These dislocations are not real dislocations in a crystalline lattice, but a mathematical device.) The state of stress induced by one of these dislocations is known—the expressions are given explicitly in Ref. 33. By applying a distribution of dislocations, of unknown density $B_r(z)$, the requirement that the crack faces be traction-free may be ensured by writing

$$0 = \tilde{\sigma}_{ij}(z, r) + \frac{G}{\pi(\kappa+1)}\int_0^c B_r(z)K(z, r)\,\mathrm{d}z \tag{4}$$

G is the shear modulus of the material, κ is Kolosov's constant (= 3–4ν in plane strain), the coordinates r, z are as in Fig. 1; the function $K(z,r)$ is given in Ref. 33. The unknown quantity, $B_r(z)$, is defined by $B_r(z) = \mathrm{d}b_r/\mathrm{d}z$, and $\tilde{\sigma}$ represents the state of stress induced by the contact in the crack's absence, i.e. in this case the radial

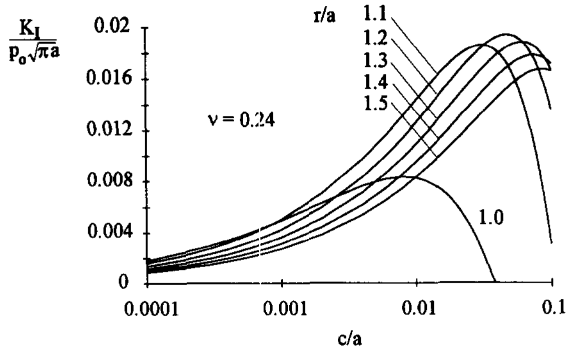

Fig. 2(a). Normalized mode I stress intensity factors as a function of normalized crack size for six normalized crack positions. Poisson's ratio = 0·24.

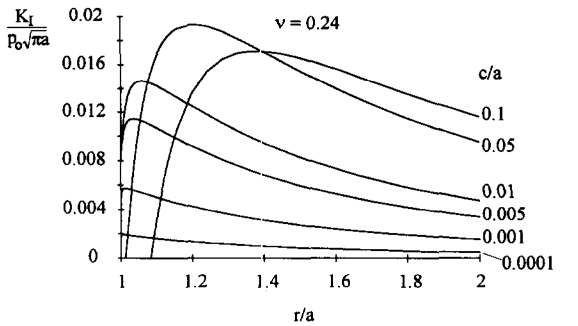

Fig. 2(b). Normalized mode I stress intensity factors as a function of normalized crack position for six normalized crack sizes. Poisson's ratio = 0·24.

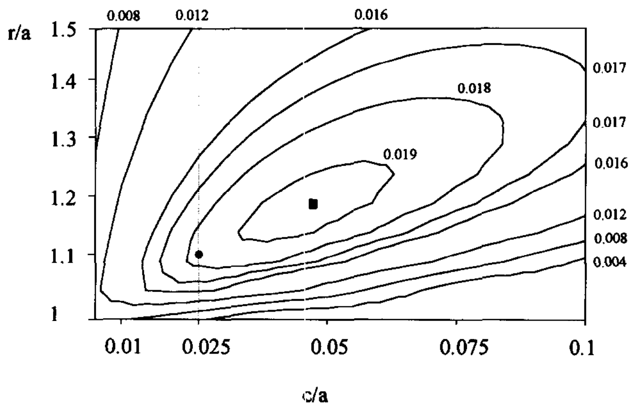

Fig. 2(c). Contours of normalized mode I stress intensity factors $K_I/(p_o\sqrt{\pi a})$ as a function of crack depth ($0{\cdot}005 < c/a < 0{\cdot}1$) and crack position ($1{\cdot}0 < r/a < 1{\cdot}5$). The filled circle shows the maximum value for $c/a = 0{\cdot}025$; at this position ($r/a \sim 1{\cdot}1$), $K_I \sim 0{\cdot}0182\ p_o\sqrt{\pi a}$. The filled square marks the position of the absolute maximum: $K_I \sim 0{\cdot}01937\ p_o\sqrt{\pi a}$ at $c/a \sim 0{\cdot}046$, $r/a \sim 1{\cdot}18$.

component of the Hertzian stress field. This integral equation is effectively represented by a set of linear algebraic equations, typically 20: the (normalized) mode I stress intensity factor can then be expressed in terms of the unknown coefficients in these linear equations. A standard computer library routine for solution of simultaneous equations is then employed. This technique is very well adapted to problems where cracks exist in a steep stress gradient. If the radial Hertzian stress ($= \tilde{\sigma}$) is expressed in terms of the peak Hertzian pressure, p_o, (eqn (3)) then the result of the calculation is a number μ which is related to the (dimensional) mode I stress intensity factor, K_I, by:

$$\mu = \frac{K_I}{p_o\sqrt{\pi c}} \quad \text{where} \quad \mu = f\left(\frac{r}{a}, \frac{c}{a}, \nu\right) \tag{5a}$$

Normalizing with respect to a (rather than c) we have:

$$\frac{K_I}{p_o\sqrt{\pi a}} = \mu\sqrt{c/a} \tag{5b}$$

The rationale for this second normalization is that the dependence of K_I on the crack size is now exclusively in the two terms on the RHS of the equation. All subsequent results presented below are in terms of this second normalization. Warren *et al.*[35] present results for the case where the sphere and the substrate are made of the same material. In this case the stress field in the substrate (and hence the values of K_I) depends on only one material parameter—Poisson's ratio of the substrate. Figures 2(a), (b) and (c) show some basic results from this analysis.

Figure 2(a) shows the normalized mode I stress intensity factor as a function of normalized crack length (c/a) for six normalized crack positions (r/a), for Poisson's ratio $= 0{\cdot}24$. Figure 2(b) shows values for the normalized K_I as a function of r/a for six values of c/a; again $\nu = 0{\cdot}24$. Figure 2(a) shows that K_I has a maximum value as a function of c/a for each r/a; furthermore for large cracks situated close to the contact radius the implied value of K_I is negative (because the crack tip is now deep enough that it lies within the compressive region of the Hertzian radial stress). Figure 2(b) shows that for each c/a the maximum in K_I occurs for $r/a > 1$. This explains the well-known fact that ring cracks are always observed to form outside the contact zone, even though the surface radial stress has its largest value at $r/a = 1$. This point has been noted previously.[16,34,36] Figure 2(c) shows a contour plot of $K_I/(p_o\sqrt{\pi a})$ as a function of crack position and crack depth (both normalized). We note two things. For each c/a, we can mark the position of the largest normalized K_I—this is shown by the filled circle for $c/a = 0{\cdot}025$. At this position ($r/a \sim 1{\cdot}1$), $K_I \sim 0{\cdot}0182 p_o\sqrt{\pi a}$); $0{\cdot}0182/\sqrt{0{\cdot}025}$ is therefore the maximum value of μ ($= \mu_{max}$) for this value of c/a, ($c/a = 0{\cdot}025$). μ_{max} is thus just a function of c/a and ν, $\mu_{max} = g(\frac{c}{a}, \nu)$. Secondly K_I has an absolute maximum—marked by the filled square, at $c/a \sim 0{\cdot}046$, $r/a \sim 1{\cdot}18$, $K_I \sim 0{\cdot}01937 p_o\sqrt{\pi a}$.

The above expressions are in terms of stress intensity factors; we will now re-write them in terms of loads. When K_I for one small surface flaw reaches K_{IC} (at a load $P = P_F$), it begins to grow—

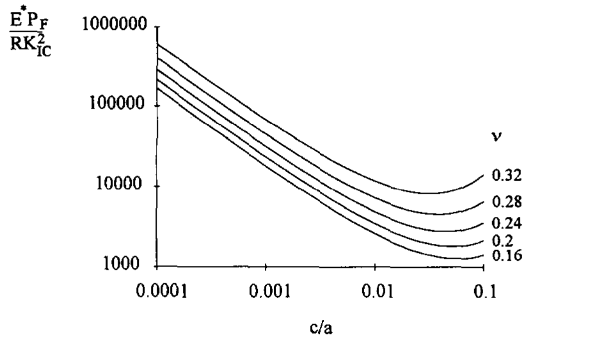

Fig. 3. Minimum normalized fracture load necessary to propagate a crack of normalized size c/a. Results for five different values of Poisson's ratio. The value of the absolute minimum for $\nu = 0{\cdot}28$ is shown.

to form either a ring crack or the well-known ring–cone system. Using eqns (1) and (3), equation (5b) becomes:

$$\frac{E^*P_F}{RK_{IC}^2} = \frac{\pi}{3\mu^2(c/a)} \tag{6}$$

We define a normalized fracture load, P_{FN}:

$$P_{FN} = \frac{E^*P_F}{RK_{IC}^2} \tag{7}$$

Assuming that the flaw distribution is dense enough so that there will always be a flaw (of size c/a) situated close to the position where the crack tip stress intensity experienced is a maximum (for this crack size) eqn (6) can be written

$$P_{FN} = \frac{\pi}{3\mu_{max}^2(c/a)} \tag{8}$$

These values of P_{FN} are therefore the minimum normalised loads necessary to propagate cracks of size c/a. Plots of P_{FN} as function of c/a (for five different values of ν) are shown in Fig. 3. For all values of Poisson's ratio there is an absolute minimum in the normalized fracture load for c/a values in the range 0·02–0·06. For a given ν, this absolute minimum in P_{FN} corresponds to the absolute maximum in $K_I/(p_o\sqrt{\pi a})$. For example, for $\nu = 0{\cdot}24$ Fig. 2(c) shows that the absolute maximum in $K_I/(p_o\sqrt{\pi a})$ is 0·01937; therefore the absolute minimum in normalized fracture load, P_{FN}^{min}, is $\pi/3/(0{\cdot}01937)^2 \sim 2790$. The values of these absolute minima and the corresponding values of c/a as a function of Poisson's ratio are shown in Fig 4 and also listed in Table 1. We emphasise that P_{FN}^{min} is a dimensionless quantity. (For all values of Poisson's ratio the absolute minimum in fracture load occurs at a relative crack position $r/a \sim 1{\cdot}20$.)

Determination of K_{IC}

The principle of the method for determining K_{IC} is now clear. For a material with a given E^* and K_{IC} one searches for the minimum value of P_F/R. If one performs a series of Hertzian tests with a sphere of given R (25 tests should be sufficient), noting the fracture loads P_F, there exists a definite minimum load for fracture, as shown in Fig. 5. If one assumes that the crack propagated in this test (by a load P_{Fmin}) is of a size within the range where P_{FN} shows a minimum with c/a then the fracture toughness can be determined from the following equation:

$$K_{IC} = \left(\frac{E^*P_{F\,min}}{P_{FN}^{min}R}\right)^{1/2} \tag{9}$$

where the number P_{FN}^{min} can be read from Table 1 assuming that Poisson's ratio for the substrate is accurately known. Similar results, but for specific r/a values (r/a = 1·05, 1·10, 1·20) were published by Matzke *et al.*[17] Since typical Hertzian contact radii are of the order of a few hundred microns (for spheres with radii 1–5 mm), to obtain the appropriate c/a values shown in Table 1 one needs flaw sizes, $c > 10\ \mu m$. Therefore the specimen surface should be prepared by coarse diamond polishing or abrasion with fine SiC grits. Severe grinding of the surface

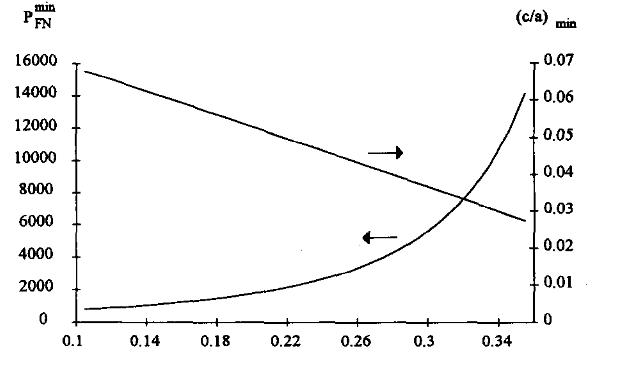

Fig. 4. Absolute minimum normalized fracture loads (P_{FN}^{min}) and the corresponding values of (c/a) as a function of Poisson's ratio.

Table 1. P_{FN}^{min} and the corresponding c/a values as a function of ν

ν	P_{FN}^{min}	$(c/a)_{min}$	ν	P_{FN}^{min}	$(c/a)_{min}$
0·10	789	0·0679	0·23	2490	0·0472
0·11	850	0·0664	0·24	2790	0·0456
0·12	917	0·0648	0·25	3131	0·0444
0·13	991	0·0632	0·26	3530	0·0423
0·14	1074	0·0616	0·27	4001	0·0407
0·15	1167	0·0600	0·28	4560	0·0391
0·16	1270	0·0584	0·29	5229	0·0374
0·17	1386	0·0568	0·30	6037	0·0357
0·18	1517	0·0553	0·31	7022	0·0341
0·19	1665	0·0537	0·32	8235	0·0324
0·20	1883	0·0521	0·33	9748	0·0307
0·21	2025	0·0504	0·34	11658	0·0290
0·22	2247	0·0488	0·35	14106	0·0273

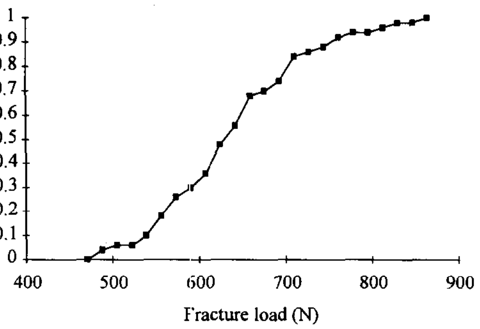

Fig. 5. Experimentally determined fracture loads, showing a minimum fracture load at P_F = 470 N. Material (substrate and sphere) — alumina; sphere radius = 2·5 mm.

may introduce flaws of suitable depth. but it is well known[37] that such treatment can introduce considerable surface residual stresses. The tests can then be repeated with spheres of different radii and the minimum value of P_{Fmin}/R found. This method requires no knowledge of the initial crack size, no measurement of the radius of the ring-crack seen on the surface after fracture, nor any measurement of the final depth of the cone-crack. It is important to note that the average fracture load found will give an overestimate of K_{IC} because not all cracks will be situated at the particular r/a value for which K_{I}, is a minimum—most cracks will be found at greater r/a values, since in reality the flaw density is not infinite.

It is appropriate here to discuss some of the limitations of this approach. With the sharp indentation method, part of the uncertainty in the analysis lies in the assumption of a particular crack geometry (median–radial or Palmqvist) after indentation. With the Hertzian method, the uncertainty lies in the value of the constant $P_{\mathrm{FN}}^{\mathrm{min}}$, which in turn depends on the assumed shape of the pre-cursor flaw before indentation. Warren *et al.*[35] assumed that the pre-cursor flaws were of a given depth c, but large in extent (with respect to the contact radius) across the surface, i.e. the sort of flaw produced by a sharp point dragged across the surface. Work is currently in progress[38] to evaluate stress intensity factors for different crack geometries, such as semi-circular or semi-elliptical flaws. The analysis presented here assumes that the sphere and the substrate are made of the same material. The method also assumes that the material does not show a substantial T-curve, i.e. increasing fracture resistance with crack extension. Finally, both the Vickers and the Hertzian method are affected by the presence of near-surface residual stresses. The Hertzian method may be particularly affected because the surface finish should specifically not be a fine diamond polish; the surface preparation method needs to be carefully chosen to produce 5–10 μm flaws without introducing residual stresses.

Table 2. Material properties

Material	ν	*E(GPa)*	P_{FN}^{min}
Glass	0·25	70	3131
Alumina	0·24	390	2790

Experimental Technique and Results

Hertzian indentation tests were performed using a modified ET500 testing machine (Engineering Systems (Nottm)*). A wide-band acoustic emission transducer was mounted in the loading train to detect the growth of a small surface flaw into the characteristic ring— or ring–cone-crack. Two different substrate materials were used—glass, and high purity (99·99%) alumina. The assumed elastic constants and the expected minimum normalised fracture load, $P_{\mathrm{FN}}^{\mathrm{min}}$, for the materials are listed in Table 2. In each case two different sphere radii were used—2·5 and 5 mm. The spheres were made of glass and alumina. The specimens had a variety of surface treatments: the alumina was either ground with 600-grit SiC slurry on a cast iron lap, or ground and then polished with 6 μm polycrystalline diamond powder; the glass was tested in the 'as received' condition, and also after grinding with 600-grit SiC. In each case about 25 tests were performed. The results are shown in Table 3 for glass and Table 4 for alumina. The average fracture loads (± one standard deviation) are also listed.

We therefore estimate the values of K_{IC} (derived from the minimum fracture loads from the SiC-abraded surfaces) to be 0·71–0·74 MPa m$^{1/2}$ for glass and 3·72–3·80 MPa m$^{1/2}$ for alumina. These values are in good agreement with those in the literature—for example Zeng *et al.*[28] found values 0·8 and 3·77 MPa m$^{1/2}$ for glass and alumina,

Table 3. Glass results

Surface treatment	*Sphere radius (mm)*	*Average fracture load (N)*	*Minimum fracture load (N)*	K_{IC} *(MPa m$^{1/2}$)*
As-received	2·5	290 ± 110	127	0·78
	5·0	638 ± 135	340	0·90
SiC grit	2·5	158 ± 95	105	0·71
	5·0	348 ± 107	231	0·74

* Engineering Systems (Nottm), 1 Loach Court, Radford Bridge Road, Nottingham NG8 INB

Table 4. Alumina results

Surface treatment	*Sphere radius (mm)*	*Average fracture load (N)*	*Minimum fracture load (N)*	K_{IC} *(MPa m$^{1/2}$)*
SiC grit	2·5	739 ± 160	470	3·72
	5·0	1600 ± 280	982	3·80
Diamond	2·5	849 ± 145	540	3·99
	5·0	1751 ± 260	1273	4·33

respectively. It can be seen that in every case the average fracture load is at least 35% bigger than the minimum load, and as expected the calculated value of K_{IC} is most accurate for the most badly damaged surface indented with the smallest sphere. This is because the more damaged the surface the larger *c/a* because of the increase in *c*; the smaller the sphere the larger *c/a* because of the reduction in *a*. In either case, the more likely it is that a crack of the appropriate size will be found.

Some of the experimental limitations are now described. (1) The crack extension must be sufficiently rapid to be detected by the acoustic emission transducer.[39] In all cases here, the detection of an acoustic signal corresponded to the appearance of a circular crack seen on the surface; in a very few cases, examination of the surface after detection of a signal revealed the presence of two ring cracks, suggesting that the first fracture event was not picked up. Because the sphere and substrate were made of identical materials, it is unlikely that cracking occurred on unloading; Johnson *et al.*[31] showed that if the substrate is more compliant than the indenter then the frictional tractions at the substrate–interface, which reduce the radial tension on loading, enhance the radial tension on unloading. (2) If an acoustic emission transducer is not available then the detection of the minimum load must be done by trial and error. (3) Obviously, the substrate must crack before the sphere does, this was not found to be a problem but the fact that it may occur suggests that tough spheres with the appropriate elastic constants (to minimise the extent of elastic mismatch between the sphere and the substrate) might be used—for instance, glass–ceramic spheres to test glass, or silicon nitride spheres to test other engineering ceramics. The effects of elastic mismatch on Hertzian fracture have been analysed,[40] the use of different indenter materials can substantially affect the value of P_{FN}^{min}.

Conclusions

Use of a refined stress intensity factor formulation for surface-breaking cracks in steep stress gradients[35] has enabled accurate estimates to be made of the minimum loads necessary to propagate cracks by Hertzian indentation. At present the analysis only applies for the case where the sphere and the substrate are made of the same material. However, the analysis is comprehensive in that it can be applied to sphere–substrate systems with any value of Poisson's ratio. By measuring this minimum load (and that is the only quantity that must be measured) an accurate estimate of K_{IC} may easily be made. The only other requirement is that the surface should be coarsely polished and a sphere of relatively small radius (<5 mm) should be used.

Two further points are worthy of note. Because the only quantity that must be measured is a fracture load, it is possible that this method of determining K_{IC} can be automated. Also, the existence of an absolute minimum fracture load, for a given sphere size, suggests that the Hertzian indentation test could find use as a localized proof-test.

Acknowledgements

The author gratefully acknowledges discussions with Professor Sir P. B. Hirsch, Dr S. G. Roberts and Dr D. A. Hills.

References

1. Sakai, M. & Bradt, R. C., Fracture toughness testing of brittle materials. *Int. Met. Rev.*, **38** (1993) 53–78.
2. Evans, A. G. & Charles, E. A., Fracture toughness determinations by indentation. *J. Am. Ceram. Soc.*, **59** (1976) 371–2.
3. Lawn, B. R., Evans, A. G. & Marshall, D. B., Elastic/plastic indentation damage in ceramics: the median/radial system. *J. Am. Ceram. Soc.*, **63** (1980) 574–81.
4. Anstis, G. R., Chantikul, P. Lawn, B. R. & Marshall, D. B., A critical evaluation of indentation techniques for measuring fracture toughness. *J. Am. Ceram. Soc.*, **64** (1981) 533–8.
5. Ponton, C. B. & Rawlings, R. D., Vickers indentation fracture toughness test—Part 1: Review of literature and formulation of standardised indentation toughness equation. *Mat. Sci. Technol.*, **5** (1989*a*) 865–72.
6. Ponton, C. B. & Rawlings, R. D., Vickers indentation fracture toughness test—Part 2: Application and critical evaluation of standardised indentation toughness equations. *Mat. Sci. Technol.*, **5** (1989*b*) 961–76.
7. Cook, R. F. & Pharr, G. M., Direct observation and analysis of indentation cracking in glasses and ceramics. *J. Am. Ceram. Soc.*, **73** (1990). 787–817.
8. Li, Z., Ghosh, A., Kobayashi, A. S. & Bradt R. C., Indentation fracture toughness of sintered silicon carbide in the Palmqvist regime. *J. Am. Ceram. Soc.*, **72** (1989) 904–11.
9. Li, Z., Ghosh, A., Kobayashi, A. S. & Bradt, R. C., Reply to Comment on Indentation fracture toughness of sintered silicon carbide in the Palmqvist regime. *J. Am. Ceram. Soc.*, **74** (1991) 889–90.
10. Srinivasan, S. & Scattergood R. O., Comment on Indentation fracture toughness of sintered silicon carbide in the Palmqvist regime. *J. Am. Ceram. Soc.*, **74** (1991) 887–8.

11. Lawn, B. R., *Fracture of Brittle Solids*, Second Edition. Cambridge University Press, Cambridge, 1993, p. 259.
12. Frank, F. C. & Lawn, B. R., On the theory of Hertzian fracture. *Proc. R. Soc. Lond.*, **A229** (1967) 291–306.
13. Powell B. D. & Tabor, D., Fracture of TiC under static and sliding contact. *J. Phys. D: Appl. Phys.*, **3** (1970) 783–8.
14. Wilshaw, T. R., The Hertzian fracture test. *J. Phys. D: Appl. Phys.*, **4** (1971) 1567–81.
15. Nadeau, J. S., Hertzian fracture of vitreous carbon. *J. Am. Ceram. Soc.*, **56** (1973) 467–72.
16. Warren, R., Measurement of the fracture properties of brittle solids by Hertzian indentation. *Acta Metall.*, **26** (1978) 1759–69.
17. Matzke Hj., Inoue, T. & Warren R., The surface energy of UO_2 as determined by Hertzian indentation. *J. Nucl. Mater.*, **91** (1980) 205–20.
18. Matzke, Hj., Hertzian indentation of thorium dioxide, ThO_2. *J. Mater. Sci.*, **15** (1980) 739–46.
19. Inoue, T. & Matzke, Hj., Temperature dependence of Hertzian indentation fracture surface energy of ThO_2. *J. Am. Ceram. Soc.*, **64** (1981) 355–9.
20. Matzke Hj. & Warren R., Hertzian crack growth in ThO_2 observed by serial sectioning. *J. Mater. Sci. Lett.*, **1**, (1982) 441–4.
21. Matzke, Hj. & Politis, C., The fracture properties of NbC, Nb(C,N) and NbN by Hertzian indentation. *Phys. Stat. Sol.*, **A69** (1982) 269–80.
22. Matzke, Hj., Meyritz, V. & Routbort, J. L., Fracture-surface energy and fracture toughness of (U,Pu)C and (U,Pu)(C,O). *J. Am. Ceram. Soc.*, **66** (1983) 183–8.
23. Laugier, M., Load bearing capacity of TiN coated WC–Co cemented carbides. *J. Mater. Sci. Lett.*, **2** (1983) 419–21.
24. Laugier, M., Hertzian indentation of sintered alumina. *J. Mater. Sci.*, **19** (1984) 254–8.
25. Laugier, M., Toughness determination of some ceramic tool materials using the method of Hertzian indentation fracture. *J. Mater. Sci. Lett.*, **4** (1985) 1542–4.
26. Laugier, M., Hertzian indentation of ultra-fine grain size WC–Co composites. *J. Mater. Sci. Lett.*, **6** (1987) 841–3.
27. Zeng, K., Breder, K. & Rowcliffe, D. J., The Hertzian stress field and formation of cone cracks—I. Theoretical approach. *Acta Metall. Mater.*, **40** (1992*a*) 2595–600.
28. Zeng, K., Breder K. & Rowcliffe D. J., The Hertzian stress field and formation of cone cracks—II. Determination of fracture toughness. *Acta Metall. Mater.*, **40** (1992*b*) 2601–05.
29. Almond, E. A., Roebuck, B. & Gee, M. G., Mechanical testing of hard materials. In *Science of Hard Materials*, Inst. Phys. Conf. Ser. Vol. 75, pp. 155–77.
30. Huber, M. T., On the theory of contacting solid elastic bodies. *Ann. Phys.*, **14** (1904) 153–63.
31. Johnson, K. L., O'Connor, J. J. & Woodward, A. C., The effect of the indenter elasticity on the Hertzian fracture of brittle materials. *Proc. R. Soc. Lond. A.*, **334** (1973) 95–117.
32. Hertz, H., On the contact of elastic solids. *Zeitschrift fur die Reine und Angewandte Mathematik*, **92** (1881) 156–71. English translation in *Miscellaneous Papers* (translated by D. E. Jones and G. A. Schott); pp. 146–62. Macmillan, London, U.K., 1896.
33. Nowell D. & Hills, D. A., Open cracks at or near free surfaces. *J. Strain Anal.*, **22** (1987) 177–84.
34. Mouginot, R. & Maugis, D., Fracture indentation beneath flat and spherical punches. *J. Mater. Sci.*, **20** (1985) 4354–76.
35. Warren, P. D., Hills, D. A. & Roberts, S. G., Surface flaw distributions and Hertzian fracture. Submitted to *J. Mater. Res.*
36. Finnie, I., Dolev, D. & Khatibloo, M., On the physical basis of Auerbach's law. *J. Engng Mater. Technol.*, **103** (1981) 183–4.
37. Marshall, D. B., Evans, A. G., Khuri-Yakub, B. T., Tien, J. W. & Kino, G. S., The nature of machining damage in brittle materials. *Proc R. Soc. Lond A.*, **385** (1982) 461–75.
38. Dai, D. N., Hills, D. A., Warren, P. D. & Nowell, D., The propulsion of surface flaws by elastic indentation testing. Accepted for publication, *Acta Metall. et. Mater.*
39. Scruby, C. B., Quantitative acoustic emission techniques. In *Research Techniques in Non-destructive Testing*, vol. 8, ed. R. S. Sharp. Academic Press, London, 1985, p. 141.
40. Warren, P. D. & Hills, D. A., The influence of elastic mismatch between indenter and substrate on Hertzian fracture. *J. Mater. Sci.*, **29** (1994) 2860–6.